Absorption effects in the expanding Universe: spectral transmittance functions of intergalactic medium for distant sources

A. Yang 1 , B. Novosyadlyj 1,2* , P. Kopach 2 , B. Melekh 2 , G. Milinevsky 1,3,4*1

We analyse the formation of troughs in the continuous spectra of sources in redshift range 5-15 for two reionization histories followed from the distant galaxy spectra and CMB anisotropy. We supposed that neutral hydrogen and helium atoms of homogeneous intergalactic medium are mainly in ground state and absorb the light of distant sources in the lines of Lyman series and continuums of HI, HeI and HeII. The frequency dependence of optical depths in the 40 lines of Lyman series of HI and HeII, and in 10 lines of HeI, as well as in their continuums were computed in order to estimate the spectral flux of radiation from halos virialized during Cosmic Dawn and Reionization epochs. Assuming the thermal continuous spectra with virialized temperature of halos with dwarf galaxy mass $\sim 10^9 \,\mathrm{M}_{\odot}$, we compute the spectral fluxes from such halos in the vicinity of our galaxy taking into account the cosmological distances, redshifts and absorptions by each absorber and all together. The obtained spectral transmittance functions of intergalactic medium, $S(\lambda;z)$, are analysed on the subject which absorber systems of HI, HeI and HeII are corresponding for formation of troughs in the continuous spectra of sources at redshift range 5-15 and how it depends on reionization history. It is shown, that spectral features in the continuous spectra of sources in redshift range 5-7 are very sensitive to the reionization histories of both elements, hydrogen and helium.

Keywords: intergalactic medium, Gunn-Peterson effect, cosmological reionization, Cosmic Dawn, spectral transmittance function

¹International Centre of Future Science and College of Physics of Jilin University, 2699 Qianjin Str., 130012, Changchun, P.R.China,

²Astronomical Observatory of Ivan Franko National University of Lviv,

⁸ Kyrylo and Methodij Str., 79005, Lviv, Ukraine,

³Department of Atmosphere Physics and Geospace, National Antarctic Scientific Center, 16 Taras Shevchenko Blvd., Kyiv 01601, Ukraine

⁴Main Astronomical Observatory of National Academy of Sciences of Ukraine, 27 Akademika Zabolotnoho Str., 03143, Kyiv, Ukraine

¹*corresponding authors

Contents

1	Observational data on the reionization history	2
2	Optical depth of the diffuse intergalactic gas in hydrogen lines and continuum	4
3	Optical depth of the diffuse intergalactic gas in the helium lines and continuum	7
4	Spectral flux from halos of Cosmic Dawn and Reionization epochs	9
5	Conclusions	14

INTRODUCTION

The Universe of the first billion years attracts the attention of investigators in order to find the answers on current challenges in cosmology and astrophysics, especially, tensions in determination of some cosmological parameters and formation of the first stars and galaxies. The epoch from the cosmological recombination ($z \approx 1090, 380 \; \text{kyr}$) up to cosmological reionization ($z \sim 6, 1 \; \text{Gyr}$) obscured by medium of neutral hydrogen and helium which absorbs the radiation of the first sources of light in a wide range of their spectra and makes them unobservable by optical telescopes. Knowledge of reionisation history of intergalactic medium can be used for constraining the models of the first sources of ionizing radiation, and contrary, the spectra of distant sources contain information about absorbers in the line of sight.

Recent high-redshift observations and cosmological simulations have significantly improved our understanding of the intergalactic medium and its thermodynamic evolution [1–5]. These advances provide new constraints on the physical conditions during the epoch of reionization and the early phases of galaxy formation, making it possible to test analytical models against detailed radiative transfer.

The cosmic microwave background radiation which penetrates the medium of Dark Ages and Reionization epochs brings the information about it in the energy spectrum and polarization. Especially, the polarization of CMB at the large angular scales measured by Planck Space Observatory [1, 2, 6] gives us the strong constraints on the fraction of free electrons, $x_{\rm e}(z)$, which is equal to fraction of ionized hydrogen in the standard Λ CDM model $x_{\rm e}(z) = x_{\rm HII}(z) = 1 - x_{\rm HI}(z)$. Another channel of information about $x_{\rm HI}(z)$ is detecting of Ly_{\alpha} line asymmetry in the spectra of sources at $z \gtrsim 5$, firstly described in [7–9]. Its complete use was made possible by the largest ground-based and space telescopes [3, 10–15]. In the last paper in Fig. 11, authors collected most current measurements of $x_{\rm HI}$ in the redshift range 5-14.

In this work, we focus on the analytical description of these processes, emphasizing their cosmological implications. The goal of this paper is analysis of formation of troughs in the spectra of distant sources caused by absorption in the Ly-series lines and continua of HI, HeI and HeII taking into account observational data on reionization history and redshift of sources in the range 5-15. For that we compute the dependence of optical depths on frequency for sources at different redshifts and illustrate impact of each absorption system

on the continuous thermal spectra of halos with mass $\sim 10^9 \text{ M}\odot$ which were virialized at redshifts 5-15.

In Section 1, we find the analytical approximations for two sets data on $x_{\rm HI}$, [15]+[3] and [15]+[6]. The dependences of optical depths in HI lines of Lyman series and continua on frequency for sources at $z \in 5-15$ are deduced in Section 2. The frequency dependences of optical depths in HeI-HeII lines of Lyman series and continua on frequency for sources at $z \in 5-15$ are deduced in Section 3. In Section 4, we model the thermal continuous spectra of virialized halos with $T=2.5\cdot 10^5$ K in their rest frame and compute the spectral fluxes from them in the vicinity of our galaxy taking into account the cosmological distances, redshifts and absorptions by each absorber and all together. The spectral transmittance functions of homogeneous intergalactic medium for sources at different z which are independent on their spectra are presented there too. Summary of analysis are presented in Conclusions.

1 Observational data on the reionization history

To study the absorption effects in the expanding Universe, which can be observable from the Earth or must be taken into account for computation of the radiation energy density during the Reionization epoch, we must assume or precalculate the number density of absorbers along the line of sight. In this paper, we approximate analytically the observational data on neutral hydrogen fraction $(x_{\rm HI})$ following from the Planck Space Observatory data on the CMB polarization at the large angular scales [2], from the Very Large Telescope high-resolution spectra of XQR-30 quasar sample which give evidence for the late end of reionization at redshift ~ 5.3 [15] and James Webb Space Telescope spectra of ~ 600 galaxies from which Kageura et al. (2025) [3] deduced the $x_{\rm HI}$ at $z \sim 6$, 7, 8–9, and 10–14. The last source presents also an excellent review of $x_{\rm HI}$ estimates from the literature using various methods, which are presented in Fig. 11 there. Here we use the estimations [15] and [3]. They are presented in the left panel of Fig. 1 as points with error bars. Also, there 2σ range of Planck constraints are shown by green lines and median values deduced by Glazer et al. (2018) [6] by red line. Two other lines are our approximation by the 5-parametric target logistic function of view

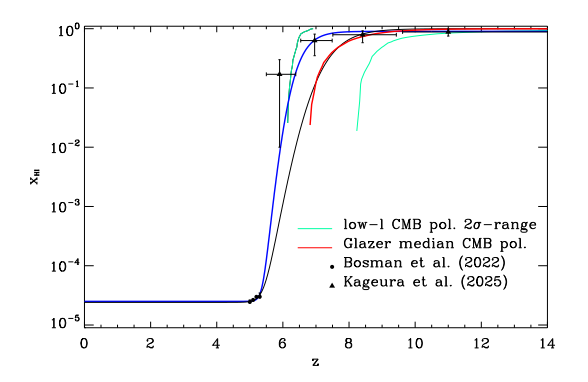
$$x_{\rm HI}(z) = a_1 + (a_2 - a_1) \left[1 + e^{\frac{a_3 - z}{a_4}} \right]^{-a_5},$$
 (1.1)

where a_i are fitting parameters. Between them, a_1 is close to fraction of neutral hydrogen at lowest redshift, a_2 is asymptotic value at largest redshift. The best-fit values of this parameters or some subset of them are determined by minimizing χ^2 using the Levenberg-Marquardt method [19] and presented in the Tab. 1.

Table 1. Best-fit values of approximation function (1.1).

No	Data	a_1	a_2	a_3	a_4	a_5
1	[15] + [3]	$2.5066 \cdot 10^{-5}$	0.90177	6.0596	0.33974	4.9822
2	[15] + [6]	$2.4115 \cdot 10^{-5}$	0.998178	6.7040	0.55658	4.5122

The approximation of [15]+[3] data show that $x_{\rm HI} \approx 0.1$, 0.5 and 0.9 are at redshift $z \approx 6.2$, 6.8 and 8.7 accordingly. The approximation of [15]+[6] data show that $x_{\rm HI} \approx 0.1$, 0.5 and 0.9 are at redshift $z \approx 6.9$, 7.7 and 8.8 accordingly. The first we call the late reionization, the second we call the early reionization. In Table 2, we present the fraction of neutral



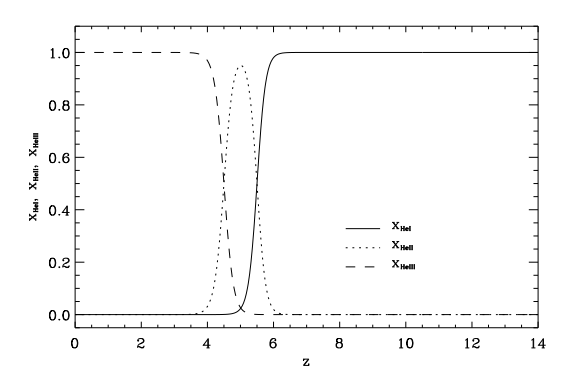


Figure 1. Evolution of the neutral fraction of hydrogen and helium atoms following from the observational data.

Table 2. Fraction of neutral hydrogen $x_{\rm HI}$ at specific redshifts $z \in 5-15$ for approximation 1 (Bosman et al. (2022) + Kageura et al. (2025) data) and 2 (Bosman et al. (2022) + Glazer et al. (2018) data).

$\overline{\mathrm{No}/z}$	5.0	5.5	6.0	6.5	7.0	8.0	10.0	12.0	15.0
1	$2.5\cdot 10^{-5}$	$1.3 \cdot 10^{-4}$	$1.8 \cdot 10^{-2}$	0.27	0.67	0.89	0.90	0.90	0.90
2	$2.5\cdot 10^{-5}$	$6.0 \cdot 10^{-5}$	$1.1 \cdot 10^{-3}$	$1.8 \cdot 10^{-2}$	0.12	0.66	0.986	0.997	0.998

hydrogen for both approximations at specific redshifts $z \in 5-15$ used in below sections.

The second important absorber in the early Universe is helium. Following the [20], we assume that it is neutral $(x_{\text{HeI}} = 1)$ at z > 6, and is doubly ionized $(x_{\text{HIII}} = 1)$ at z < 4. We approximate their z-dependences as $x_{\text{HeI}} = (1 + \tanh y_1)/2$ and $x_{\text{HeIII}} = (1 + \tanh y_2)/2$ with $y_1 = (1 + z)^{3/2} - 16.58$ and $y_2 = 12.90 - (1 + z)^{3/2}$ accordingly. Then the fraction of single ionized helium at any z is $x_{\text{HeII}} = 1 - x_{\text{HeII}} - x_{\text{HeIII}}$. They are shown in the right panel of Fig. 1.

Our approximations can be used for computations of z-dependence of the free electrons fraction, $x_e(z) = n_e(z)/n_{\rm H}$, where $n_e(z) = n_{\rm H}(0)(1-x_{\rm HI}(z))(1+z)^3 + n_{\rm He}(0)(x_{\rm HeII}(z) + 2x_{\rm HeIII}(z))(1+z)^3$. It gives us the possibility to estimate the goodness of our approximation by computing the optical depth caused by Thomson scattering of radiation by free electrons,

$$\tau_{\rm Th}(z_{\rm s}) = n_{\rm H}(0)c\sigma_{\rm T} \int_0^{z_{\rm s}} dz \, \frac{x_{\rm e}(z)(1+z)^2}{H_0\sqrt{\Omega_{\rm m}(1+z)^3 + \Omega_{\Lambda}}},$$
(1.2)

(c is the speed of light, $\sigma_{\rm T}$ is cross-section of Thomson scattering) and compare it with Planck data [1] (Tab. 7). For $H_0=67.36~{\rm km/s/Mpc}$, $\Omega_{\rm m}=0.3153$, $\Omega_{\rm b}=0.0493$ and $\Omega_{\Lambda}=0.6847$ we have $n_{\rm H}(0)=2.0178\cdot 10^{-7}~{\rm cm^{-3}}$, $n_{He}=1.5357\cdot 10^{-8}~{\rm cm^{-3}}$. The results are presented in Table 3. Both estimations of τ for z=15 are in the 1σ range of value, obtained in [1] for the $\Lambda{\rm CDM}$ model with the same cosmological parameters: 0.0544 ± 0.0073 . But this Planck value is given for z=50. In the last column, we present $\tau_{\rm Th}$ for $z_{\rm s}=50$. We can see, that the first approximation gives strongly overestimated value, while the second one well agree with Planck Collaboration result 2018. It also means that approximation 1 can not be continued out the range of its applying.

Table 3. Optical depth for Thomson scattering to sources at specific redshifts $z \in 5-15$ for approximation 1 (Bosman et al. (2022) + Kageura et al. (2025) data) and 2 (Bosman et al. (2022) + Glazer et al. (2018) data).

No/z	5.0	5.5	6.0	6.5	7.0	8.0	10.0	12.0	15.0	50.0
1	0.028	0.032	0.036	0.040	0.042	0.044	0.046	0.048	0.051	0.112
2	0.028	0.032	0.036	0.041	0.045	0.050	0.052	0.052	0.052	0.053

2 Optical depth of the diffuse intergalactic gas in hydrogen lines and continuum

Since the goal of our paper is analysis of transmission of continuous spectra of the first sources of light from the Cosmic Dawn and Reionization epochs we do not need to know the real spectra of sources. It is enough to assume some spectral energy distribution or spectral luminosity, to take into account the cosmological redshift, define absorbers, their spectral lines and to integrate the equations of radiative transfer for the specific intensity I_{ν} in the lines along the line of sight. The most comfortable for this aims are thermal spectra describing the Planck function with unique parameter temperature. The most of astrophysical objects have the energy distributions which can be roughly approximated by Planck function with some temperature and spectral features. By such objects in the early Universe can be Pop III stars, virialised halos, proto-galaxies, globular clusters or dwarf galaxies.

In the previous paper [16] we studied the impact of the cosmological expansion on the continuum thermal spectra of distant sources assuming empty space between them. In this paper we study the impact of the absorption of the expanding intergalactic medium on the continuous spectra of the first sources of light. We assume that hydrogen and helium atoms in the intergalactic medium are mainly in the ground state, since the number density of atoms and energetic electromagnetic quanta are too low at $z \leq 14$ to make statistically important populations of the excited levels.

Table 4. The wavelengths $\lambda_{1-n}^{\text{HI}}$ and oscillator strengthens f_{1-n}^{HI} for the first 39 hydrogen lines of Lyman series [21].

<u> Ly man</u>	berreb [21].							
1-n	$\lambda_{ m 1-n}^{ m HI}$	$f_{ m 1-n}^{ m HI}$	1-n	$\lambda_{ m 1-n}^{ m HI}$	$f_{ m 1-n}^{ m HI}$	1-n	$\lambda_{ m 1-n}^{ m HI}$	$f_{1-\mathrm{n}}^{\mathrm{HI}}$
1-2	1215.67	0.41641	1-15	915.821	0.00046886	1-28	912.916	7.1476E-05
1-3	1025.720	0.079142	1-16	915.327	0.00038577	1-29	912.837	6.4319E-05
1-4	972.537	0.029006	1-17	914.917	0.00032124	1-30	912.765	5.8087E-05
1-5	949.743	0.013945	1-18	914.574	0.00027035	1-31	912.701	5.2635 E-05
1-6	937.803	0.0078035	1-19	914.284	0.000229671	1-32	912.642	4.7845 E-05
1-7	930.748	0.0048164	1-20	914.036	0.00019677	1-33	912.589	4.3619E-05
1-8	926.223	0.0031850	1-21	913.823	0.00016987	1-34	912.541	3.9877E-05
1-9	923.148	0.0022172	1-22	913.639	0.00014767	1-35	912.496	3.6551E-05
1-10	920.961	0.0016062	1-23	913.478	0.00012917	1-36	912.455	3.3585E-05
1-11	919.349	0.0012011	1-24	913.337	0.00011364	1-37	912.418	3.0931E-05
1-12	918.127	0.0009219	1-25	913.212	0.00010051	1-38	912.383	2.8550E-05
1-13	917.178	0.0007231	1-26	913.102	8.9321E-05	1-39	912.351	2.6407E-05
1-14	916.427	0.00057769	1-27	913.004	7.9736E-05	1-40	912.321	2.4474E-05

We analyse here the hydrogen (HI) and helium (HeI and HeII) absorption in the lines

of Lyman series and Lyman-continuum. The expression for optical depth in the Ly_{α} line for cosmological sources was obtained by Gunn & Peterson in 1965 [9]. We generalize it for all lines considered here and for any set of cosmological parameters.

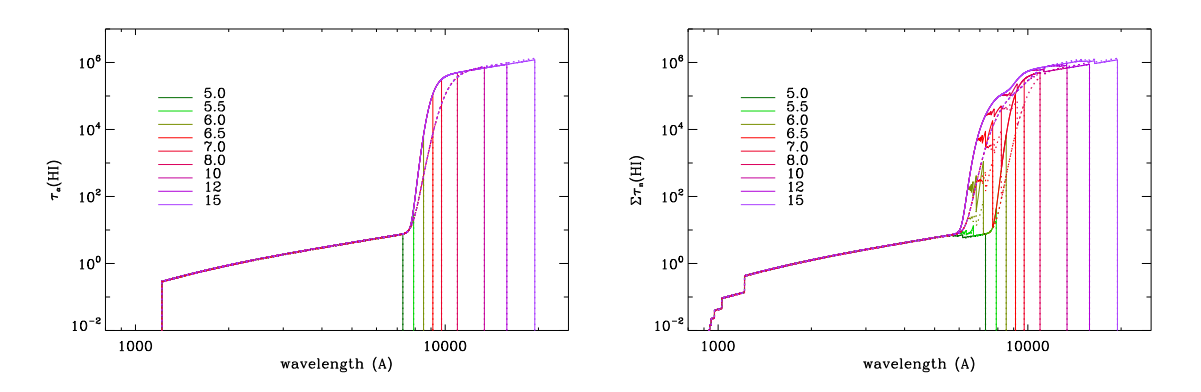


Figure 2. Optical depth in the Ly_{α} line (left panel) and superposition of the first 39 lines of Lyman series of HI (right panel) for the sources at different redshifts.

The effective cross-section of absorption in the Ly $_{\alpha}$ line is

$$\sigma_{\alpha}^{\rm HI}(\nu, z) = \alpha_{fs} \frac{h_{\rm P}}{2m_e} f_{\alpha}^{\rm HI} \Phi_{\alpha}(\nu; b, z), \tag{2.1}$$

where $\alpha_{fs} = 7.2973525698 \times 10^{-3}$ is the fine structure constant, $h_{\rm P}$ is Planck constant, m_e is electron mass, $f_{\alpha}^{\rm HI} = 0.4164$ is the oscillator strength of the transition, and Φ_{α} is profile of Ly_{α} line. The last can be approximated by Voigt profile [17, 18]:

$$\Phi_{\alpha}(\nu, z) \approx \frac{1}{b_{\nu}\sqrt{\pi}} \left[\frac{A}{\sqrt{\pi}(A^2 + B^2)} + e^{-B^2} \right], \quad A = \frac{A_{21}}{4\pi b_{\nu}}, \quad B = \frac{\nu(1+z)/(1+z_0) - \nu_{\alpha}}{b_{\nu}}, \quad (2.2)$$

where $b_{\nu} = \frac{b\nu_{\alpha}}{c}$ is the frequency width of the line and $b = \sqrt{\frac{2k_BT_b(z)}{m_H}} + b_{turb}^2$ is rms velocity caused by thermal and bulk turbulent motions of the hydrogen atoms in the intergalactic medium. Observations support the thermal broadening of lines with $T_{\rm b} \lesssim 2 \cdot 10^4$ K at the end of reionization. So, the range of redshift Δz in which the coming continuum radiation are absorbed by local neutral hydrogen does not exceed $\sim 5 \cdot 10^{-4}$, is very narrow. Since the integral $\int_{-\infty}^{+\infty} \Phi_{\alpha}(\nu, z) d\nu/\nu_{\alpha} = 1$, the expression for optical depth in this line in the Λ CDM model has analytical form as follows

$$\tau_{\alpha}^{\text{HI}}(\nu, z) = \frac{c}{H_0} \int_{z_0}^{z_{\text{s}}} \frac{n_{\text{HI}}(z) \sigma_{\alpha}^{\text{HI}}(\nu, z) dz}{(1+z) \cdot \sqrt{\Omega_{\text{m}} \cdot (1+z)^3 + \Omega_{\Lambda}}}
= 9.194 \cdot 10^{10} \lambda_{\alpha}^{\text{HI}} f_{\alpha}^{\text{HI}} (1-Y_{\text{p}}) \frac{\Omega_{\text{b}} h (1+z)^3 x_{\text{HI}}(z)}{\sqrt{\Omega_{\text{m}} (1+z)^3 + \Omega_{\Lambda}}},$$
(2.3)

which for $z\gg 1$ and known atomic constants become the same $\tau_{\rm GP}^{\rm HI}$ as in [12, 13]. In the last part of expression, the redshift along of line of sight is related with wavelength as $z=(1+z_{\rm s})\lambda_{\alpha}^{\rm HI}/\lambda-1$, where $\lambda_{\alpha}^{\rm HI}\leq\lambda\leq\lambda_{\alpha}^{\rm HI}(1+z_{\rm s}),\,z_{\rm s}$ is the redshift of source and $z_{\rm o}$ is the redshift of observer. In this paper all computations are carried out for $z_{\rm o}=0$.

The expression (2.3) can be easy generalized for Ly_{β} , Ly_{γ} and so on by substitutions of corresponding wavelengths and oscillator strengthens

$$\tau_{\rm Ly_n}^{\rm HI}(z) = 9.194 \cdot 10^{10} \lambda_{\rm 1-n}^{\rm HI} f_{\rm 1-n}^{\rm HI} (1 - Y_{\rm p}) \frac{\Omega_{\rm b} h (1+z)^3 x_{\rm HI}(z)}{\sqrt{\Omega_{\rm m} (1+z)^3 + \Omega_{\Lambda}}}, \quad z = (1+z_{\rm s}) \frac{\lambda_{\rm 1-n}^{\rm HI}}{\lambda} - 1. \quad (2.4)$$

In our computations we use the first 39 lines of Lyman series for which the values of wavelengths $\lambda_{1-n}^{\rm HI}$ and oscillator strengthens $f_{1-n}^{\rm HI}$ are taken from [21]. They are collected in the Table 4. A superficial look at the values of these quantities suggests that only a few of the lowest energy levels of the Lyman series are important in terms of influencing the observed spectrum of distant light sources. Here we will show which ones should be taken into account in the appropriate calculations.

In the left panel of Fig. 2, we present the dependence of $\tau_{\alpha}^{\rm HI}$ on the wavelength for sources at different redshifts for both approximations of $x_{\rm HI}(z)$, presented in Fig. 1 (solid line for approximation 1, dotted line for 2). One can see, that for both approximations $\tau_{\alpha}^{\rm HI} > 1$ for z > 5 and $\lambda \gtrsim 2000$ Å. Equations (2.3)-(2.4) shows that,

$$\tau_{\rm Ly_n}^{\rm HI}(\lambda;z) \propto \tau_{\alpha}^{\rm HI} \frac{\lambda_{\rm 1-n}^{\rm HI} f_{\rm 1-n}^{\rm HI}}{\lambda_{\alpha}^{\rm HI} f_{\alpha}^{\rm HI}}.$$
(2.5)

It gives the possibility to estimate the importance of taking into account other lines of Lyman series. At $z\approx 6$, the optical depth is lower than 1 only in the lines with transitions from the ground base level to 25 one and higher. For sources at higher redshifts, the optical depths in all 39 lines of Lyman series are essentially large then 1. In the right panel we show the superposition of the first 39 lines of Lyman series $\tau_{\rm Ly}^{\rm HI}=\Sigma_2^{39}\tau_{\rm Lyn}^{\rm HI}$ for the sources at different redshifts.

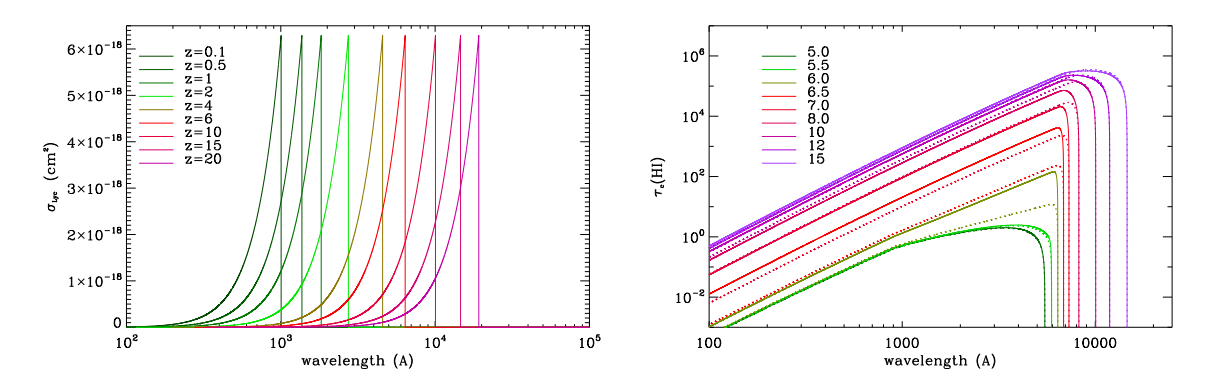


Figure 3. The frequency dependences of the effective cross-section of absorption in the Lyman-continuum in the rest frame of Earth observer transferred from the source reference system at different redshifts (left) and optical depth for distant sources at different redshift (right) for both approximations of $x_{\rm HI}$ (1 - solid line, 2 -dotted one).

The experimental measurements of the effective cross-section in the Lyman-continuum

according to [22–24] can be approximated as follows

$$\sigma_{\rm c}^{\rm HI}(\nu, z) = \begin{cases} 1.1083 \cdot 10^{-14} \frac{(E/E_0 - 1)^2 (E/E_0)^{-4.31275}}{(1 + \sqrt{E/E_0/23.424})^{2.3745}}, & \nu \frac{1+z}{1+z_0} \ge \nu_{\rm pi} \\ 0, & \nu \frac{1+z}{1+z_0} < \nu_{\rm pi} \end{cases}$$
(2.6)

where $\nu_{\rm pi}=3.288\cdot 10^{15}$ Hz ($\lambda_{\rm pi}^{\rm HI}=911.75$ Å) is frequency (wavelength) corresponded to the potential of ionization of atomic hydrogen $E_{\rm pi}=13.6\,{\rm eV}$, and $E_0=1.0235\,{\rm eV}$ is constant of approximation. The frequency dependences of the effective cross-section (2.6) in the rest frame of Earth observer transferred from the source reference system at different redshifts by relation $\nu_{\rm pi}^{\rm o}=\nu_{\rm pi}(1+z_{\rm o})/(1+z_{\rm s})$ are shown in the left panel of Fig. 3.

The optical depth in this case is integral

$$\tau_{\rm c}^{\rm HI}(\nu,z) = \frac{cn_{\rm H}^0}{H_0} \int_{z_{\rm o}}^{z_{\rm s}} \frac{x_{HI}(z)(1+z)^2 \sigma_{\rm c}^{\rm HI}(\nu,z) dz}{\sqrt{\Omega_m (1+z)^3 + \Omega_L}}, \quad \text{where} \quad n_{\rm H}^0 = (1-Y_{\rm P}) \frac{\Omega_{\rm b}}{m_{\rm H}} \frac{3H_0^2}{8\pi G}. \quad (2.7)$$

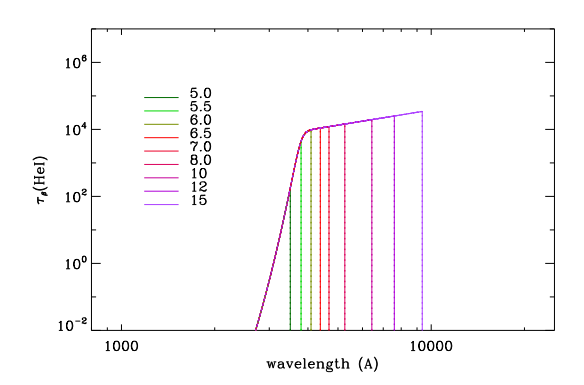
Its frequency dependence for the distant sources at different redshift for both approximations of $x_{\rm HI}$ (1st - solid line, 2nd -dotted one) is presented in the right panel of Fig. 3. One can see, that near potential of ionization the optical depth $\tau_{\rm c}^{\rm HI}(\lambda \lesssim \lambda_{\rm pi}^{\rm HI} > 1$ for $z \gtrsim 5$, and is huge for $z \gtrsim 6$. We note also essentially lower optical depths for sources at $z \approx 6-8$ for the 2nd approximation of $x_{\rm HI}$ in comparison with the 1st one. So, the spectral features there can be different too. In the far ultraviolet range, the intergalactic medium has optical depth < 1 up to z = 15.

3 Optical depth of the diffuse intergalactic gas in the helium lines and continuum

The assumed here the reionization history of helium, shown in the right panel of Fig. 1, illustrates that at $z \gtrsim 6$ helium is neutral like hydrogen and doubly ionized at $z \lesssim 4$. It means that number density of photons with energy large than potential of ionisation HeI and HeII increased in spite of expansion of the Universe. So, the spectral features caused by HeI and HeII absorptions in the continuous spectra of the distant objects can be present. In order to analyse this we estimate in this section the optical depths of intergalactic medium in the lines of base series (Lyman) of HeI atoms and HeII ions.

Table 5. The wavelengths $\lambda_{1-n}^{\text{HeI}}$ and oscillator strengthens f_{1-n}^{HeI} for the first 10 HeI lines of Lyman series [21].

1-n	$\lambda_{ m 1-n}^{ m HeI}$	$f_{ m 1-n}^{ m HeI}$	1-n	$\lambda_{ m 1-n}^{ m HeI}$	$f_{1-\mathrm{n}}^{\mathrm{HeI}}$
1-2	591.412	2.77500E-08	1-7	512.099	0.0086306
1-3	584.334	584.334	1-8	509.998	0.0054073
1-4	537.030	0.07346	1-9	508.643	0.0036108
1-5	522.213	0.029873	1-10	507.718	0.0025304
1-6	515.617	0.015045	1-11	507.058	0.0018420



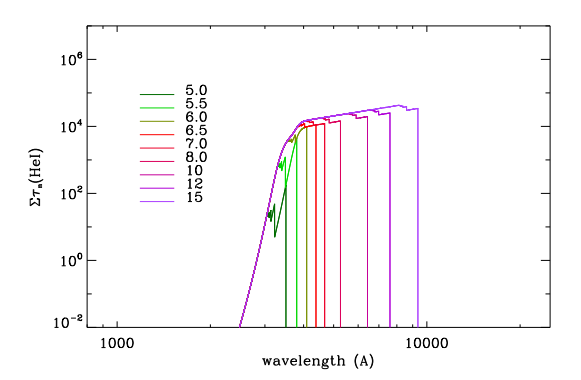


Figure 4. Optical depth in the Ly_{β} line (left panel) and superposition of the first 10 lines of Lyman series of HeI (right panel) for the sources at different redshifts.

By the similar way as for hydrogen, one can deduce the expression for optical depth in the lines of Lyman series of neutral helium atoms HeI,

$$\tau_{\rm Ly_n}^{\rm HeI} = 2.2985 \cdot 10^{10} \lambda_{\rm 1-n}^{\rm HeI} f_{\rm 1-n}^{\rm HeI} Y_{\rm p} \frac{\Omega_{\rm b} h (1+z)^3 x_{\rm HeI}(z)}{\sqrt{\Omega_{\rm m} (1+z)^3 + \Omega_{\Lambda}}}, \quad z = (1+z_{\rm s}) \frac{\lambda_{\rm 1-n}^{\rm HeI}}{\lambda} - 1. \tag{3.1}$$

The values of wavelengths and oscillator strengths for the first 10 Lyman lines of HeI taken from [21] are presented in Tab. 5. The transition 1-2 is dipole forbidden partially by quantum selection rules and its oscillator strength is small. So, the absorption in it is small too. In the left panel of Fig. 4, we present the dependence of $\tau_{\beta}^{\rm HeI}$ on the wavelength for sources at different redshifts and in the right panel the superposition of the first 10 lines of Lyman series of HeI. One can see, that $\tau_{\beta}^{\rm HeI} \gg 1$ for z > 5 and $\lambda \gtrsim 3000$ Å.

The optical depth in the Lyman continuum of HeI atoms is as follows

$$\tau_{\rm c}^{\rm HeI}(\nu,z) = \frac{cn_{\rm He}^0}{H_0} \int_{z_0}^{z_{\rm s}} \frac{x_{HeI}(z)(1+z)^2 \sigma_{\rm c}^{\rm HeI}(\nu,z) dz}{\sqrt{\Omega_m (1+z)^3 + \Omega_L}}, \quad \text{where} \quad n_{\rm He}^0 = Y_{\rm P} \frac{\Omega_{\rm b}}{m_{\rm He}} \frac{3H_0^2}{8\pi G}. \quad (3.2)$$

The approximation for effective cross-section of absorption in the HeI Lyman continuum is as follows [25]

$$\sigma_{\rm c}^{\rm HeI} = 7.4 \cdot 10^{-18} \left[a_1 x^{-s} + (1 - a_1) x^{-(s+1)} \right] + \frac{7.33 \cdot 10^{-22}}{E(keV)^{7/2}} \left[1 + a_2 x^{-1/2} e^{-a_3 x^{-1/2}} \right], \quad (3.3)$$

where x=E/24.58 eV, $E=h_{\rm P}\nu$, $a_1=7.3861$, s=3.9119, $a_2=-3.2491$, $a_3=1.1783$. It is shown in the left panel of Fig. 5. In the right panel, we present the optical depths in HeI Lyman continuum for sources at different redshifts. One can see, that $\tau_{\rm c}^{\rm HeI}>1$ on $\lambda\gtrsim700$ Å for sources at $z_{\rm s}=5$, on $\lambda\gtrsim220$ Å for sources at $z_{\rm s}=5.5$ and $\lambda_{\tau_{\rm c}^{\rm HeI}=1}(z_{\rm s})$ quickly decreases with increasing $z_{\rm s}$.

We compute the optical depths in the lines of Lyman series and continuum of ionised helium atoms using the hydrogen atomic data, since HeII is hydrogen like ion: $\lambda_{ij}^{\rm HeII} = \lambda_{ij}^{\rm HI}/4$, $f_{ij}^{\rm HeII} = f_{ij}^{\rm HI} \mu^{\rm HI}/\mu^{\rm HeII}$, $\mu^{\rm HI}/\mu^{\rm HeII} \approx 0.9996$. The results of computations are presented in Fig. 6.

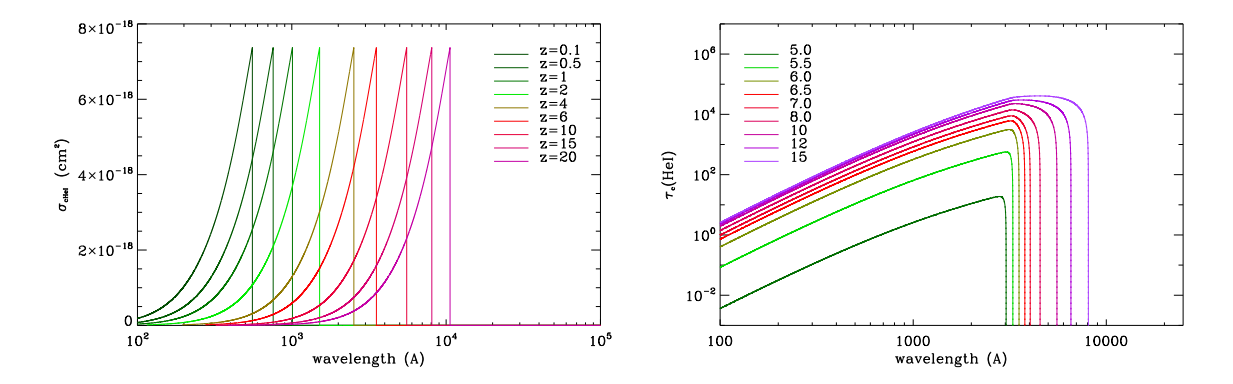


Figure 5. The frequency dependences of the effective cross-section of absorption in the HeI Lyman-continuum in the rest frame of Earth observer transferred from the source reference system at different redshifts (left) and optical depth in the HeI Lyman-continuum for distant sources at different redshift (right).

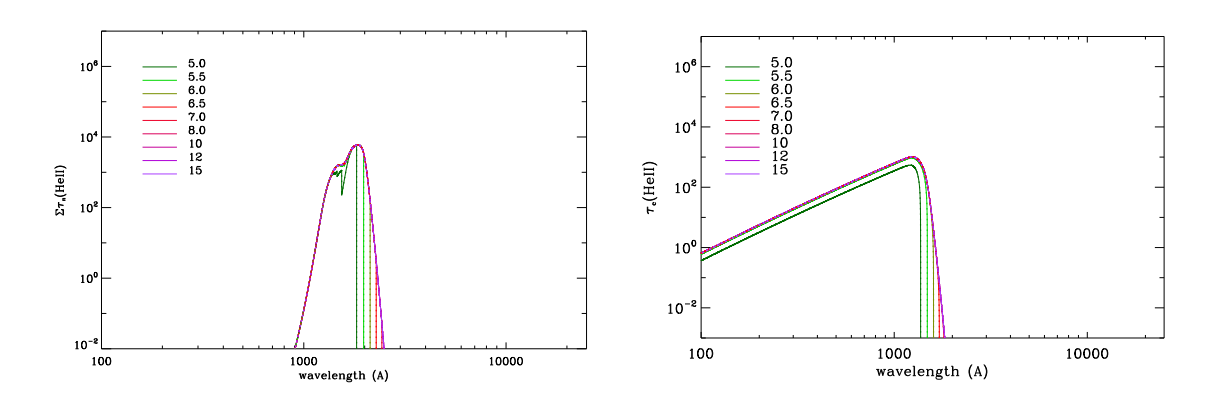


Figure 6. The optical depths in the HeII lines of Lyman series (superposition of 39 lines, left panel) and in Lyman-continuum (right panel) for distant sources at different redshift.

4 Spectral flux from halos of Cosmic Dawn and Reionization epochs

In this section, we analyse how each absorption system, described in the previous section, and all together change the continuous spectra of sources, which are at the redshift range $5 \le z \le 15$. We assume the reionization histories which are presented by two analytical approximations in Section 2 and suppose the thermal continuous spectrum of sources. In computations, we assume that such sources are virialized spherical halos with temperatures [26, 27],

$$T = 2 \cdot 10^4 \left(\frac{\mu_{\rm H}}{1.2}\right) \left(\frac{M_{\rm h}}{10^8 \,{\rm M}_{\odot}}\right)^{2/3} \left(\frac{\Delta_{\rm vir}}{178}\right)^{1/3} \left(\frac{z_{\rm vir} + 1}{10}\right) \,{\rm K},\tag{4.1}$$

where $\mu_{\rm H}$ is mass per H atom, $z_{\rm vir}$ is redshift of halo virialization, and $\Delta_{\rm vir}$ is density contrast at the moment of virialization. The halo mass $M_{\rm h}/M_{\odot}$ and its comoving radius $R_{\rm h}/{\rm kpc}$ after virialization are related as [24]

$$R_{\rm h} = 1.5 \left[\left(\frac{M_{\rm h}}{10^8 M_{\odot}} \right) \frac{178}{\Delta_{\rm vir}} \frac{0.143}{\Omega_{\rm m} h^2} \right]^{1/3} \frac{10}{1 + z_{\rm vir}} \quad \text{kpc.}$$
 (4.2)

These relations show, that in the standard Λ CDM model the halos with $M_{\rm h} \sim 10^9 - 10^{10} M_{\odot}$ at redshifts 5-15 have temperatures in the range $(2-7)\cdot 10^5$ K and radius in the range (2-17) kpc. Kageura et al. (2025) assume that massive halos are the primary sources of reionization.

To analyse the influence of the absorption systems considered above on the continuous spectrum of distant sources of radiation, we assume that halos at different redshifts have the same temperature, and set it equal to $2.5 \cdot 10^5$ K. For simplicity, we set $z_{vir} = z_{\rm s}$.

Let's estimate the spectral flux from halo of such mass at different redshifts assuming that it is homogeneous, optically thin and continuum spectrum is caused by free-free and free-bound transitions. Recent refinements of the classical free-free emission formalism have been developed using high-precision quantum mechanical calculations and modern numerical fits [28–30]. These studies provide updated Gaunt factors and radiative coefficients over a wide parameter range, which enables a more accurate modelling of early-Universe plasma conditions. Our approach follows the same physical principles but applies them to a different cosmological regime, emphasizing the analytic transparency of the resulting expressions. The angle-integrated emissivity of plasma in the rest frame of source according to [31–34] is as follows

$$\epsilon_{\nu} = 6.8 \cdot 10^{-38} Z^2 (g_{\rm fb} + g_{\rm ff}) n_{\rm e} n_{\rm i} T^{-1/2} \exp\left(-\frac{h_{\rm P} \nu}{k_{\rm B} T}\right) \left[\frac{\rm erg}{\rm s \cdot cm^3 \cdot Hz}\right],$$
 (4.3)

where Z is mean charge of particles in plasma, $g_{\rm fb}$ and $g_{\rm ff}$ are Gaunt factors for free-bound and free-free transitions. For completely ionized hydrogen-helium plasma $Z\approx 1.07$, product of number density of electrons and ions for such plasma $n_{\rm e}n_{\rm i}\approx 1.26n_{\rm H}^2$. In this range of frequencies and temperatures $g_{\rm fb}\approx 1$ and $g_{\rm ff}\approx 1.2$ [32]. The spectral luminosity in the rest frame of source is $L_{\nu_{\rm (s)}}=\frac{4}{3}\pi R_{\rm h}^3\epsilon_{\nu_{\rm (s)}}$ and the spectral flux at the observer

$$F_{\nu_{(o)}}(z_s) = \frac{L_{\nu_{(s)}}}{4\pi D_L^2} e^{-\tau(z_s)}$$
(4.4)

where $\nu_{(s)} = \nu_{(o)}(1+z_s)$ and the luminosity distance of source D_L is related with its redshift by well known relationship

$$D_{\rm L}(z_{\rm s}) = \frac{c}{(1+z_{\rm s})H_0} \int_0^{z_{\rm s}} \frac{dz}{\sqrt{\Omega_{\rm m}(1+z)^3 + \Omega_{\Lambda}}}.$$
 (4.5)

The masses and radii of the halos used in the illustrative calculations are given in Table 6. In the last column, we present the estimations of the spectral fluxes from halos at different redshift at 3 μ m for comparison with sensitivity of JWST. According to [35], it can detect a flux of 18.9 nJy at $\lambda \approx 3 \,\mu$ m with signal-to-noise ratio S/N=10 for the integration time 10000 s. It means that fluxes from such halos and diffuse component of protogalaxies are essentially lower than JWST sensitivity.

The results of computations of spectral fluxes in the range $100 \le \lambda \le 30000$ Å from the halos at redshifts $5 \le z \le 15$ for discussed absorbers are presented in Figs. 7-8. In the upper left panel of Fig. 7, the spectral fluxes without absorption are presented for comparison. The following panels successively show the effect of absorption in the Ly_{\alpha} line, superposition of Lyman lines, in the Lyman continuum, and total absorption by HI, HeI, and HeII separately, and, finally, all together (the lowest right panel in Fig. 8).

We can divide an arbitrary spectral flux in each panel with absorption in Figs. 7-8 by the spectral flux without absorption for corresponding redshifts (upper-left panel in Fig. 7)

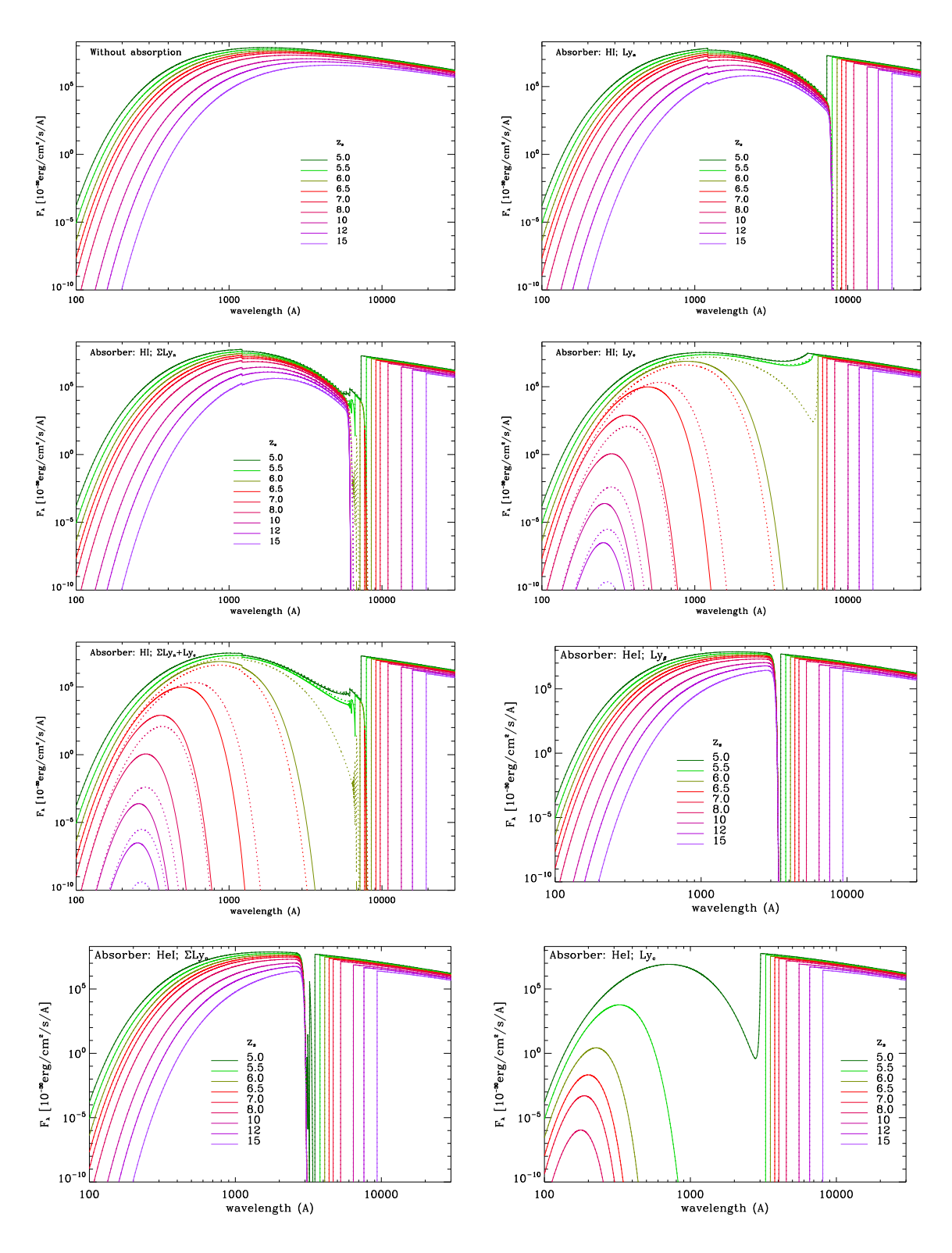


Figure 7. Absorption features caused by HI, HeI and HeII atoms in the spectral flux of halos with $T_{\rm vir} = 2.5 \cdot 10^5$ K at different redshifts.

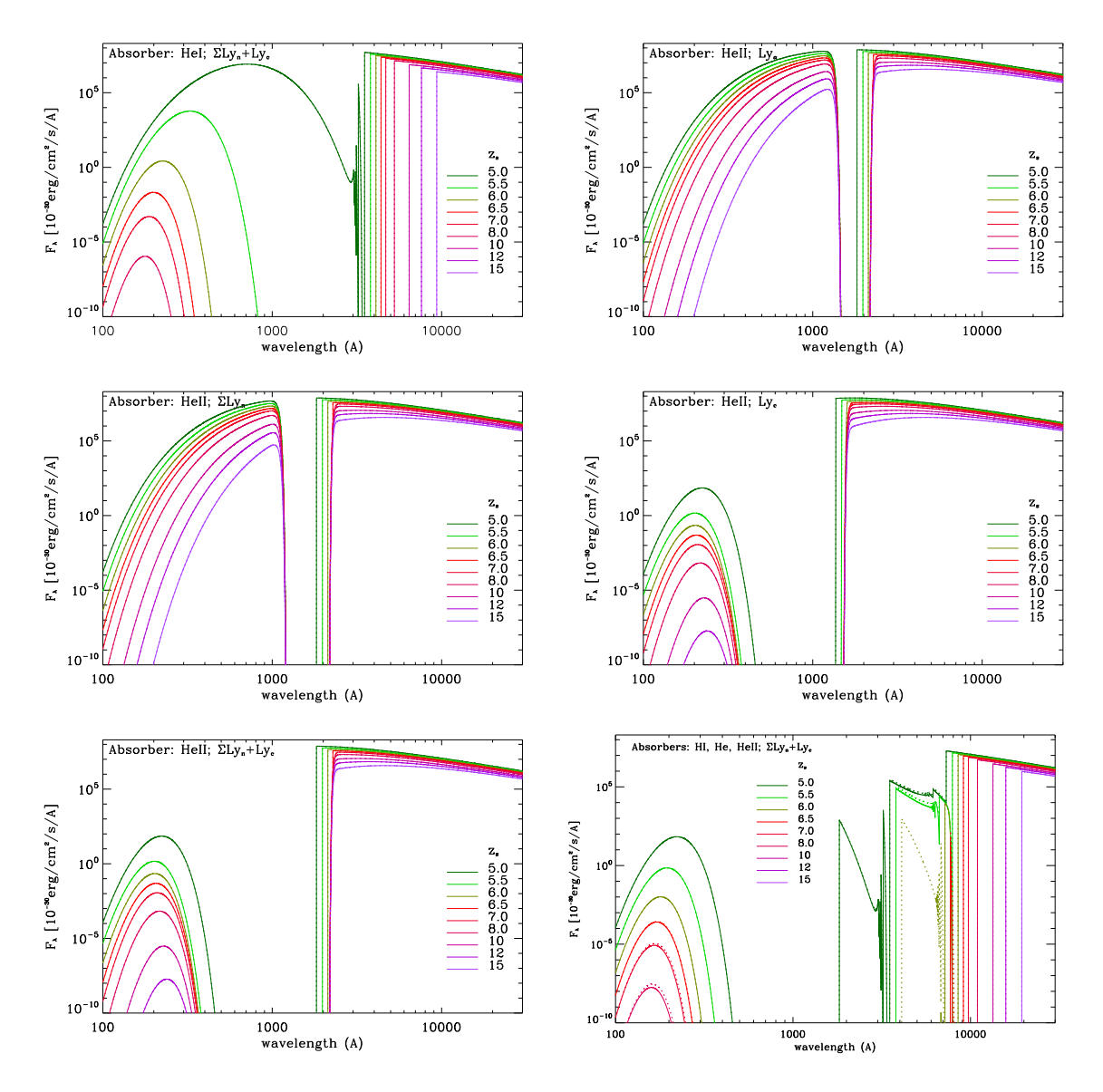


Figure 8. (continue) Absorption features caused by HI, HeI and HeII atoms in the spectral flux of halos with $T_{\rm vir} = 2.5 \cdot 10^5$ K at different redshifts.

and obtain the spectral transmittance functions $S(\lambda; z_s)$ for different absorbers at different redshifts, which does not depend on spectrum of source,

$$S(\lambda; z_{\rm s}) \equiv \frac{F_{\lambda}(\tau(z_{\rm s}))}{F_{\lambda}(\tau(z_{\rm s}) = 0)} = e^{-\tau(z_{\rm s})}.$$
(4.6)

In Fig. 9, we present the spectral transmittance functions of intergalactic medium for absorption by HI, HeI, HeII and HI+HeI+HeII. It illustrates the formation of deep troughs in the spectra of distant sources caused by absorption in the lines of Lyman series and Lyman continuum of HI, HeI and HeII. All absorbers are important for interpretation of observable spectra of sources at redshifts large than 4. One can see that the width of general trough increases with redshift of source and at the level of 10^{-2} is between 224 - 3506 Å for source

Table 6. Masses, radii and spectral fluxes at 3 μ m from halos with virialised temperature $2.5 \cdot 10^5$ K at redshift range 5-15.

$z_{ m s}$	$M_{ m h}/M_{\odot}$	$R_{\rm h}~({\rm kpc})$	$F_{\nu}(3\mu\mathrm{m})\;(\mathrm{nJy})$
5.0	$9.4 \cdot 10^9$	11.4	0.049
5.5	$8.3 \cdot 10^9$	10.0	0.044
6.0	$7.5 \cdot 10^9$	9.0	0.040
6.5	$6.7 \cdot 10^9$	8.1	0.036
7.0	$6.1 \cdot 10^9$	7.4	0.033
8.0	$5.1 \cdot 10^9$	6.2	0.029
10.0	$3.8 \cdot 10^9$	4.6	0.023
12.0	$3.0 \cdot 10^9$	3.6	0.018
15.0	$2.2 \cdot 10^9$	2.6	0.014

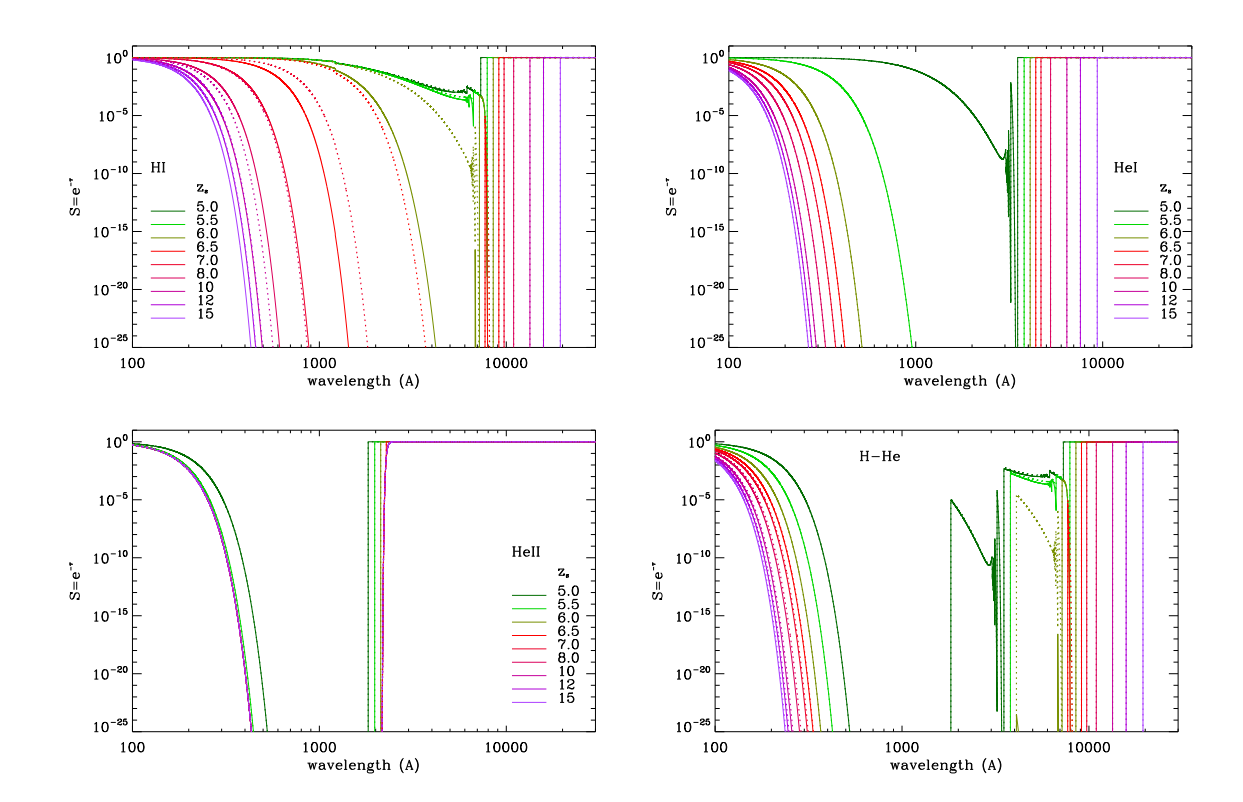


Figure 9. Spectral transmittance function for absorption by HI (upper left panel), HeI (upper right panel), HeII (bottom left panel) and HI+HeI+HeII (bottom right panel).

at z=5, 160-8717 Å for source at z=6, 137-9734 Å for source at z=7, 126-10941 Å for source at z=8, 115-13384 Å for source at z=10, 111-13384 Å for source at z=12 and 107-19467 Å for source at z=15. The JWST Near Infrared Spectrograph (NIRSpec) cowers wavelength range 6000-53000 Å [35]. In the total spectral transmittance functions (bottom right panel) we included also the Thomson scattering, which lowers the entire spectrum of the source at $z_{\rm s}=15$ by $\sim 5\%$, and for sources at $z_{\rm s}=5$ by $\sim 2.8\%$ for both approximations. The different reionization histories in the redshift range $z\in 5.5-15$

(Table 2) result into difference z-dependence of Thomson optical depth within $\sim 1\%$ only (Table 3). It is not visible in the log-log Fig. 9.

5 Conclusions

The reionization history deduced from the JWST spectra of ~ 600 galaxies [3] and from the Very Large Telescope high-resolution spectra of XQR-30 quasar sample [15] well agrees with constraints following from the SO Planck [1, 2] data on low harmonic polarization of CMB. The optical depth caused by Thomson scattering of radiation on free electrons computed with approximation of data [3] together with data on quasar spectra at z > 5 [15] is $\tau(z_{\rm s} = 15) = 0.051$ for approximation 1 and 0.052 for approximation 2. But, $\tau(z_{\rm s} = 50) = 0.112$ for 1st approximation and 0.053 for 2nd one against 0.0544 \pm 0.0073 [1]. It means that in the model of reionization with 1st approximation the sharp decreasing of $x_{\rm e}$ up to $\sim 10^{-3} - 10^{-4}$ at $z \gtrsim 15$ must be added to not contradict with Planck data.

To analyse the impact of variation of line-of-sight reionization history on the continuous spectra of sources at $z \geq 5$, we computed the optical depth in the lines of Lyman series and continuum of HI, HeI and HeII in the homogeneous intergalactic medium. The results presented in Figs. 2-6 show that $\tau(\lambda;z) \gg 1$ to sources at $z \geq 5$ in the lines of Lyman series in the range ~ 5500 Å $-\lambda_{Ly\alpha}^{\rm HI}(1+z_{\rm s})$ for HI, ~ 3000 Å $-\lambda_{Ly\alpha}^{\rm HeI}(1+z_{\rm s})$ for HeI, and ~ 1800 Å-2200 Å for HeII. The last range is defined by the redshift range 4-6 where helium is mainly single ionized. It means existence of deep Gunn-Peterson troughs in these spectral range with sharp edges. The optical depths in the Lyman continua of HI, HeI, and HeII shift the left walls of the troughs toward shorter wavelengths and makes them less sharp.

The formation of Gunn-Peterson troughs in the HI, HeI and HeII Lyman lines and continua is modeled for the thermal free-free and free-bound spectra of virialized halos at $5 \le z \le 15$ with mass $2-9 \cdot 10^9$ M_{\odot} and temperature $2.5 \cdot 10^5$ K (Figs. 7-8). The spectral transmittance functions of intergalactic medium (Fig. 9) illustrate the trough caused by absorption of HI, HeI and HeII and all together. They can be used for spectra of any sources corrected for cosmological redshifts and luminosity distances (Fortran90 code is available at https://github.com/luspav/spectral-transfer-function-hhe). The width of general trough increases with redshift of source and at the level of 10^{-2} is 3282 Å for source at z=5, 13273 Å for source at z=10 and 19360 Å for source at z=15. The variation of the reionization history of the hydrogen in the 2σ -range of Planck data results change notably the continuous spectra of sources at $z \in 5.5-6.5$.

The results presented here prove the importance of each absorption system of H and He analysed here in the formation of Gunn-Peterson trough(s) in the continuous spectra of sources at $z \gtrsim 4$.

Acknowledgements

This work was supported by the International Center of Future Science and College of Physics of Jilin University (P.R.China). PK and BM thank National Research Foundation of Ukraine (grant 2023.03/0098) for support of their part of contribution.

References

- [1] Planck Collaboration: Y. Akrami, F. Arroja, M. Ashdown et al., *Planck 2018 results. I. Overview, and the cosmological legacy of Planck*, Astron. Astrophys. **641** (2020) A1. doi: 10.1051/0004-6361/201833880
- [2] Planck Collaboration: N. Aghanim, Y. Akrami, M. Ashdown et al., Planck 2018 results. VI. Cosmological parameters, A&A 641 A6; doi: 10.1051/0004-6361/201833910
- [3] Y. Kageura, M. Ouchi, M. Nakane et al., Census of Ly_{α} Emission from ~ 600 Galaxies at z=5-14: Evolution of the Ly_{α} Luminosity Function and a Late Sharp Cosmic Reionization, Astroph. J. Suppl. S. **278** (2025) 33; https://doi.org/10.3847/1538-4365/adc690
- [4] N.Y. Gnedin, & A.A. Kaurov, Modeling of the cosmological ionizing background with radiative transfer simulations, Astroph. J. **793** (2014) 30. doi:10.1088/0004-637X/793/1/30
- [5] E. Puchwein, F. Haardt, M.G. Haehnelt & P. Madau, Consistent modelling of the metagalactic UV background and the thermal/ionization history of the intergalactic medium, Mon. Not. Roy. Astron. Soc. 485 (2019) 47. doi:10.1093/mnras/stz222
- [6] Glazer D., Rau M. M. and Trac H., The Reionization Parameter Space Consistent with the Thomson Optical Depth from Planck Research, Notes of the American Astronomical Society 2 (2018) 135; 10.3847/2515-5172/aad68a
- [7] Shklovsky, I. S. 1964, Astron. Zh., 41, 408
- [8] P.A.G. Scheuer, A Sensitive Test for the Presence of Atomic Hydrogen in Intergalactic Space, Nature, 207 (1965) 963
- [9] J.E. Gunn, B.A. Peterson, On the Density of Neutral Hydrogen in Intergalactic Space., Astroph. J. 142 (1965) 1633; doi: 10.1086/148444
- [10] X. Fan, R.L. White, M. Davis, R.H. Becker, M.A. Strauss et al. The Discovery of a Luminous Z=5.80 Quasar from the Sloan Digital Sky Survey Astron. J. 120 (2000) 1167; 10.1086/301534
- [11] X. Fan, V.K. Narayanan, R.H. Lupton, M.A. Strauss, G.R. Knapp et al. A Survey of z > 5.8 Quasars in the Sloan Digital Sky Survey. I. Discovery of Three New Quasars and the Spatial Density of Luminous Quasars at $z \sim 6$ Astron. J. **122** (2001) 2833; 10.1086/324111
- [12] R. H. Becker, X. Fan, R. L. White et al., Evidence for reionization at $z \sim 6$: Detection of a gunn-peterson trough in a z = 6.28 quasar, Astron. J. 122 (2001) 2850 doi:10.1086/324231
- [13] X. Fan, V. K. Narayanan, M. A. Strauss et al., Evolution of the ionizing background and the epoch of reionization from the spectra of $z \sim 6$ quasars, Astron. J. **123** (2002) 1247 doi: 10.1086/339030
- [14] L. Pentericci, X. Fan, H.-W. Rix, M.A. Strauss, V.K. Narayanan et al. *VLT Optical and Near-Infrared Observations of the z* = 6.28 *Quasar SDSS J1030+0524*, Astron. J. **123** (2002) 2151; 10.1086/340077
- [15] S. E. I. Bosman, F. B. Davies, G. D. Becker et al., Hydrogen reionization ends by z = 5.3: Lyman-α optical depth measured by the XQR-30 sample, Mon. Not. Roy. Astron. Soc. 514 (2022) 55; https://doi.org/10.1093/mnras/stac1046
- [16] A. Yang, B. Novosyadlyj, G. Milinevsky, Impact of the cosmological expansion on spectral energy density of radiation in the intergalactic medium and once more about Olbers' paradox, J. Phys. Stud. 29 (2025) 1901; https://doi.org/10.30970/jps.29.1902
- [17] W. Voigt, Uber die Intensit atsverteilung innerhalb einer Spectrallinie, Phys. Zeits. 14 (1913) 377
- [18] V. Iršič, M. McQuinn, Absorber Model: the Halo-like model for the Lyman-α forest, Journal of Cosmology and Astroparticle Physics **04** (2018) 026; 10.1088/1475-7516/2018/04/026

- [19] W.H. Press, B.P. Flannery, S.A. Teukolsky, W.T. Vettrling, Numerical recipes in FORTRAN. New York: Cambridge Univ. Press, (1992).
- [20] M. Kuhlen and C.-A. Faucher-Giguère Concordance models of reionization: implications for faint galaxies and escape fraction evolution, Mon. Not. Roy. Astron. Soc. 423 (2012) 862; doi:10.1111/j.1365-2966.2012.20924.x
- [21] W. L. Wiese, J. R. Fuhra, Accurate Atomic Transition Probabilities for Hydrogen, Helium, and Lithium, Phys. Chem. Ref. Data 38 (2009) 565 doi: https://doi.org/10.1063/1.3254213
- [22] D. A. Verner, G. J. Ferland, K. T. Korista, D. G. Yakovlev, Atomic data for astrophysics. I. Radiative recombination rates for H-like, He-like, Li-like, and Na-like ions over a broad range of temperature, Astron. J. 465 (1996) 487 doi: 10.1086/192284
- [23] R.P. Bauman, G.J. Ferland, K.B. MacAdam, Open Source codes for H-like ions' atomic transition probabilities, photoionization cross-sections, and radiative recombination rate coefficients, Bulletin of the American Astronomical Society 33 (2012) 1331
- [24] B. Novosyadlyj, Yu. Kulinich, B. Melekh V. Shulga, The first molecules in the intergalactic medium and halos of the Dark Ages and Cosmic Dawn, A&A 663 (2022) A120 doi:10.1051/0004-6361/202243238
- [25] M. Yan, H. R. Sadeghpour, A. Dalgarno, Photoionization cross sections of He and H_2 M, Astroph. J. 496 (1998) 1044 doi:10.1086/305420
- [26] R. Barkana, A. Loeb, In the beginning: the first sources of light and the reionization of the universe, Phys. Rep. 349 (2001) 125 10.1016/S0370-1573(01)00019-9
- [27] V. Bromm, N. Yoshida, The First Galaxies, Ann. Rev. A&A, 49 2011) 373 10.1146/annurev-astro-081710-102608
- [28] P.A.M. van Hoof, R.J.R. Williams, K. Volk, M. Chatzikos & G.J. Ferland, Accurate determination of the free-free Gaunt factor I: Non-relativistic case, Mon. Not. Roy. Astron. Soc. 444 (2014) 420;
- [29] J. Chluba, A. Ravenni & B. Bolliet, Thermal bremsstrahlung and cosmological recombination radiation. Mon. Not. Roy. Astron. Soc. **492** (2020) 177;
- [30] J. Pradler & L. Semmelrock, Non-relativistic electron-ion bremsstrahlung: an approximate formula for all parameters, Astroph. J. **922** (2021) 57.
- [31] K.R. Lang, Astrophysical formulae. A Compendium for the Physicist and Astrophysicist, Springer-Verlag, Berlin - Heidelberg - New York (1974)
- [32] Rybicki, G. B. & Lightman, A. P. (1979), Radiative Processes in Astrophysics, Wiley-VCH
- [33] Spitzer, L. (1978), Physical Processes in the Interstellar Medium*, Wiley-Interscience
- [34] Draine, B. T. (2011), Physics of the Interstellar and Intergalactic Medium*, Princeton Univ.
- [35] Space Telescope Science Institute (STScI). (2023). JWST Near-Infrared Camera (NIRCam) imaging sensitivity [Online documentation]. Retrieved October 31, 2025, from https://jwst-docs.stsci.edu/jwst-near-infrared-camera/nircam-performance/nircam-sensitivity